Since January 2020 Elsevier has created a COVID-19 resource centre with free information in English and Mandarin on the novel coronavirus COVID-19. The COVID-19 resource centre is hosted on Elsevier Connect, the company's public news and information website.

Virus Research 222 (2016) 1–12

Contents lists available at ScienceDirect

Virus Research

journal homepage: www.elsevier.com/locate/virusres

JNK and p38 mitogen-activated protein kinase pathways contribute to porcine epidemic diarrhea virus infection

Changhee Lee*, Youngnam Kim, Ji Hyun Jeon

Animal Virology Laboratory, School of Life Sciences, BK21 Plus KNU Creative BioResearch Group, Kyungpook National University, Daegu 702-701, Republic of Korea

ARTICLE INFO

Article history:
Received 3 March 2016
Received in revised form 17 May 2016
Accepted 18 May 2016
Available online 20 May 2016

Keywords:
PEDV
p38 MAPK
JNK1/2
Signal transduction
Viral replication

ABSTRACT

The mitogen-activated protein kinase (MAPK) pathways, which are central building blocks in the intracellular signaling network, are often manipulated by viruses of diverse families to favor their replication. Among the MAPK family, the extracellular signal-regulated kinase (ERK) pathway is known to be modulated during the infection with porcine epidemic diarrhea virus (PEDV); however, involvement of stress-activated protein kinases (SAPKs) comprising p38 MAPK and c-Jun NH_2-terminal kinase (JNK) remains to be determined. Therefore, in the present study, we investigated whether activation of p38 MAPK and JNK cascades is required for PEDV replication. Our results showed that PEDV activates p38 MAPK and JNK1/2 up to 24 h post-infection, whereas, thereafter their phosphorylation levels recede to baseline levels or even fall below them. Notably, UV-irradiated inactivated PEDV, which can enter cells but cannot replicate inside them, failed to induce phosphorylation of p38 MAPK and JNK1/2 suggesting that viral biosynthesis is essential for activation of these kinases. Treatment of cells with selective p38 or JNK inhibitors markedly impaired PEDV replication in a dose-dependent manner and these antiviral effects were found to be maximal during the early times of the infection. Furthermore, direct pharmacological inhibition of p38 MAPK or JNK1/2 activation resulted in a significant reduction of viral RNA synthesis, viral protein expression, and progeny release. However, independent treatments with either SAPK inhibitor did not inhibit PEDV-induced apoptotic cell death mediated by activation of mitochondrial apoptosis-inducing factor (AIF) suggesting that SAPKs are irrelevant to the apoptosis pathway during PEDV infection. In summary, our data demonstrated critical roles of the p38 and JNK1/2 signaling pathways in facilitating successful viral infection during the post-entry steps of the PEDV life cycle.

1. Introduction

Porcine epidemic diarrhea virus (PEDV) is a highly contagious and deadly enterotropic swine coronavirus that causes acute enteritis with high mortality rates in neonatal piglets (Debouck and Pensaert, 1980; Lee, 2015). PEDV infection is characterized by severe villous atrophy in the small intestine that results in watery diarrhea followed by fatal dehydration in newborn pigs (Lee, 2015; Pensaert and de Bouck, 1978; Saif et al., 2012). PEDV was first identified as the etiological agent of porcine epidemic diarrhea (PED) in Belgium in 1978 (Pensaert and de Bouck, 1978). Thereafter, it appeared in several European countries and Asia (Pensaert et al., 1981; Takahashi et al., 1983). Although PEDV remained fairly rare in Europe for some time, it continued to cause serious epizootics in Asia, thereby posing an economic threat to swine-producing nations in the last two decades (Chen et al., 2008; Kweon et al., 1993; Lee and Lee, 2014; Li et al., 2012; Lin et al., 2014; Puranaveja et al., 2009; Sun et al., 2012; Suzuki et al., 2015). At present, however, the menace of PEDV is not limited to Asia but extends worldwide, leading to significant financial concerns in the global pork industry, since the virus first emerged in the United States in 2013 (Stevenson et al., 2013) and re-emerged throughout Western and Central Europe in 2014 (Boniotti et al., 2016; Grasland et al., 2015; Hanke et al., 2015; Mesquita et al., 2015; Steinrigl et al., 2015; Theuns et al., 2015).

PEDV is a member of the genus *Alphacoronavirus* within the family *Coronaviridae* of the order *Nidovirales* (Pensaert and de Bouck, 1978; Lee, 2015). PEDV is a large, enveloped virus that possesses a single-stranded positive-sense RNA genome approximately 28 kb long with a 5′ cap and a 3′ polyadenylated tail (Pensaert and de Bouck, 1978; Saif et al., 2012). The PEDV genome includes a

* Corresponding author at: School of Life Sciences, College of Natural Sciences, Kyungpook National University, Daegu, 41566 Republic of Korea.
E-mail address: changhee@knu.ac.kr (C. Lee).

http://dx.doi.org/10.1016/j.virusres.2016.05.018
0168-1702/

5′ untranslated region (UTR), at least seven open reading frames (ORF1a, ORF1b, and ORFs 2–6), and a 3′ UTR (Kocherhans et al., 2001). The two large ORFs (ORF1a and ORF1b) that occupy two-thirds of the 5′-proximal genome encode non-structural proteins (nsps). The remaining ORFs in the 3′-proximal genome region code for four major structural proteins, the 150–220 kDa glycosylated spike (S), 20–30 kDa membrane (M), 7 kDa envelope (E), and 58 kDa nucleocapsid (N) proteins, and one accessory gene ORF3 (Duarte et al., 1994; Lai et al., 2007; Lee, 2015). PEDV replication begins with the interaction of the viral S protein with the receptor on host cells followed by entry of the virus via direct fusion with the membrane. After the uncoating process, the viral genome is released into the cytosol and functions as mRNA for the synthesis of viral proteins. Initial ORF1a translation yields replicase polyprotein (pp) la, whereas the ORF1b product is expressed by means of a −1 ribosomal frame shift (RFS), which C-terminally extends ppla into pp1ab. Subsequently, the two polyproteins are cleaved post-translationally by internal proteases, resulting in 16 functional nsps including the viral RNA-dependent RNA polymerase (RdRp). The RdRp-containing replicase complex then engages in replication of viral genomic RNA and transcription of subgenomic (sg) mRNA. The latter generates a nested set of 3′ co-terminal sg mRNAs that are finally translated into structural proteins (Lai et al., 2007; Lee, 2015).

Perception of various extracellular stimuli by cells, e.g., viral infection, activates specific intracellular signaling networks such as the mitogen-activated protein kinase (MAPK) cascade pathways. As central regulators of responses to changes in external conditions, the MAPK pathways transmit signals to the intracellular environment and control a variety of cellular activities in a coordinated fashion. Three distinct MAPKs have been identified, and their well-characterized pathways are named after the respective terminal MAPK components: extracellular signal-regulated kinases (ERK), p38 MAPK, and c-Jun N-terminal kinases (JNK) (Roux and Blenis, 2004; Shaul and Seger, 2007; Sui et al., 2014). JNK and p38 MAPK are also referred to as stress-activated protein kinases (SAPKs) because they are activated by bacterial toxins, environmental stressors, and proinflammatory cytokines (Roux and Blenis, 2004; Tibbles and Woodgett, 1999). Upon stimulation, cell surface receptors are engaged to send signals for activation of MEK3/6 and MEK4/7, upstream dual activators, which in turn phosphorylate p38 MAPK and JNK, respectively. JNK and p38 MAPK that are activated by phosphorylation eventually are translocated into the nucleus where they phosphorylate numerous downstream substrates, including transcription factors, thereby modulating transcription of a large number of genes involved in various cellular processes. Thus, the p38 MAPK and JNK pathways control a wide range of key cellular functions such as cell proliferation, differentiation, and apoptosis (Dong et al., 2002; Roux and Blenis, 2004; Sui et al., 2014).

Because viruses entirely depend on host cells to complete their life cycle, they have coevolved with their hosts to adjust pre-existing intracellular signal transduction networks, including the MAPK cascades, to benefit their own multiplication. In fact, many viruses are known to stimulate MAPKs after binding, entry, or replication and to exploit the host pathways in order to regulate cellular or viral gene expression or both for the success of viral replication (Georgopoulou et al., 2003; Greber, 2002; Huang et al., 2011; Lee and Lee, 2010, 2012; Lim et al., 2005; Marjuki et al., 2006; Mori et al., 2003; Pan et al., 2006; Rahaus et al., 2004; Schümann and Dobbelstein, 2006; Si et al., 2005; Wang et al., 2006; Wei and Liu, 2009; Wei et al., 2009; Yu et al., 2009; Zampieri et al., 2007). Recently, we also demonstrated that the ERK signaling pathway is activated by PEDV replication to promote the development of viral infection (Kim and Lee, 2015). Nevertheless, the role of other MAPK family members, in particular p38 MAPK and JNK, in PEDV replication has not been determined. In the present study, therefore, we sought to investigate whether PEDV has an ability to activate the p38 MAPK and JNK cascades in cultured cells and whether their activation, in turn, affects PEDV replication. It was found that infectious PEDV induces progressive activation of both p38 MAPK and JNK, judging by their higher phosphorylation levels up to 36 h postinfection (hpi). In contrast, ultraviolet (UV) light-inactivated PEDV could not trigger phosphorylation of SAPKs, indicating that active viral multiplication is responsible for their activation. PEDV production was notably diminished by treatment of cells with either a p38 inhibitor or JNK inhibitor. Further experiments revealed that suppression of p38 MAPK or JNK1/2 activation by the SAPK inhibitors had no effect on viral entry but greatly impaired biosynthesis of viral RNAs and proteins. In addition, inhibition of SAPK activation did not affect PEDV-induced apoptotic cell death. Collectively, our data demonstrate significant functions of the p38 MAPK and JNK signaling pathways at the post-attachment stages of the PEDV life cycle.

2. Materials and methods

2.1. Cells, viruses, reagents, and antibodies

Vero cells were cultured in alpha minimum essential medium (α-MEM; Invitrogen, Carlsbad, CA) with 5% fetal bovine serum (FBS; Invitrogen) and antibiotic-antimycotic solutions (100×; Invitrogen). The cells were maintained at 37 °C in a humidified 5% CO_2 incubator. PEDV strain SM98-1 was kindly provided by the Korean Animal and Plant Quarantine Agency and propagated in Vero cells as described previously (Hofmann and Wyler, 1988; Nam and Lee, 2010). Inactivation of PEDV was performed by UV irradiation of the virus suspension with 1000 mJ/cm^2 using a UV crosslinker (Stratagene, La Jolla, CA). Virus inactivation was confirmed by the inoculation of the UV-treated virus on Vero cells followed by N protein-specific staining as described below, and the inactivated virus was stored at −80 °C. The p38 MAPK inhibitor SB202190 and the JNK inhibitor SP600125 were purchased from Sigma (St. Louis, MO). The PEDV N protein-specific monoclonal antibody (MAb) was obtained from ChoogAng Vaccine Laboratory (CAVAC; Daejeon, South Korea). Antibodies specific for p38, JNK1/2, and their phosphorylated forms (p-p38 and p-JNK1/2) were obtained from Cell Signaling Technology (Danvers, MA). The anti-AIF and anti-β-actin antibodies and horseradish peroxidase (HRP)-conjugated secondary antibodies were purchased from Santa Cruz Biotechnology (Santa Cruz, CA).

2.2. Cell viability assay

The cytotoxic effects of reagents on Vero cells were analyzed using a colorimetric 3-(4,5-dimethylthiazol-2-yl)-2,5-diphenyltetrazolium bromide (MTT) assay (Sigma, St Louis, MO) to detect cell viability. Briefly, Vero cells were grown at 1×10^4 cells/well in a 96-well tissue culture plate with SB202190 or SP600125 treatment for 24 h. After 1 day of incubation, 50 μl of MTT solution (1.1 mg/ml) was added to each well, and the samples were incubated for an additional 4 h. The supernatant was then removed from each well, after which 150 μl of DMSO was added to dissolve the colored formazan crystals produced by the MTT. The absorbance of the solution was measured at 540 nm using an enzyme-linked immunosorbent assay plate reader. All MTT assays were performed in triplicate.

2.3. Western blot analysis

Vero cells were grown in 6-well tissue culture plates for 1 day and were mock infected or infected with PEDV at a multiplicity of infection (MOI) of 1 or with an equal amount of UV-inactivated

virus. At the indicated times, cells were harvested in 50 μl of lysis buffer (0.5% TritonX-100, 60 mM β-glycerophosphate, 15 mM ρ-nitro phenyl phosphate, 25 mM MOPS, 15 mM $MgCl_2$, 80 mM NaCl, 15 mM EGTA [pH 7.4], 1 mM sodium orthovanadate, 1 μg/ml E64, 2 μg/ml aprotinin, 1 μg/ml leupeptin, and 1 mM PMSF) and sonicated on ice 5 times for 1 s each. Homogenates were lysed for 30 min on ice, and clarified by centrifugation at 15,800*g* (Eppendorf centrifuge 5415R, Hamburg, Germany) for 30 min at 4 °C. To examine the effect of p38 MAPK or JNK inhibition on PEDV replication, cells were pretreated independently with SB202190 or SP600125 and then infected with PEDV at an MOI of 1. The virus-inoculated cells were further propagated in the presence of SB202190 (5–10 μM), SP600125 (1–5 μM), or DMSO (0.5%; vehicle control) and cell lysates were prepared with lysis buffer at 48 h hpi. The total protein concentrations in the supernatants were determined using a BCA protein assay (Pierce, Rockford, IL). Equal amounts of total protein were separated on a NuPAGE 4–12% gradient Bis-Tris gel (Invitrogen) under reducing conditions and electrotransferred onto an Immobilon-P (Millipore, Bedford, MA). The membranes were subsequently blocked with 3% powdered skim milk (BD Biosciences, Bedford, MA) in TBS (10 mM Tris–HCl [pH 8.0], 150 mM NaCl) with 0.05% Tween-20 (TBST) at 4 °C for 2 h and incubated at 4 °C overnight with the primary antibody against p-p38, p38, p-JNK1/2, JNK1/2, PEDV N, or β-actin. The blots were then incubated with the corresponding secondary HRP-labeled antibodies at a dilution of 1:5000 for 2 h at 4 °C. Proteins were visualized using enhanced chemiluminescence (ECL) reagents (GE Healthcare, Piscataway, NJ) according to the manufacturer's instructions. Ratios of phosphorylated/total p38 or JNK1/2 were compared by densitometry of the corresponding bands using a computer densitometer with the Wright Cell Imaging Facility (WCIF) version of the ImageJ software package (http://www.uhnresearch.ca/facilities/wcif/imagej/). To quantify viral protein production, the band densities of PEDV N proteins were quantitatively analyzed using a computer densitometer with ImageJ software in terms of the density value relative to that of the β-actin gene.

2.4. Immunofluorescence assay (IFA)

Vero cells grown on microscope coverslips placed in 6-well tissue culture plates were mock infected or infected with PEDV or UV-inactivated PEDV at an MOI of 1 for the indicated times. To assess the effect of SAPK inhibitors on PEDV infection, cells were pretreated with SB202190, SP600125, or DMSO for 1 h and then infected with PEDV. Virus-infected cells were subsequently maintained in the presence of vehicle or each inhibitor for 48 h. All treated cells were fixed with 4% paraformaldehyde for 10 min at RT and permeabilized with 0.2% Triton X-100 in PBS at RT for 10 min. The cells were blocked with 1% bovine serum albumin (BSA) in PBS for 30 min at RT and then incubated with PEDV N-specific MAb for 2 h. After being washed five times in PBS, the cells were incubated for 1 h at RT with a goat anti-mouse secondary antibody conjugated to Alexa Fluor 488 (Invitrogen), followed by counterstaining with 4′,6-diamidino-2-phenylindole (DAPI; Sigma). The coverslips were mounted on microscope glass slides in mounting buffer and cell staining was visualized using a fluorescent Leica DM IL LED microscope (Leica, Wetzlar, Germany). To examine AIF subcellular localization under the chemical inhibition of PEDV-induced SAPK activation, MitoTracker Red CMXRos (200 nM; Invitrogen) was added to vehicle or each SAPK inhibitor-treated and virus-infected Vero cells and left for 45 min at 37 °C prior to fixation. The cells were then stained with AIF-specific antibody as described above, and cell staining was analyzed using a Confocal Laser Scanning microscope (Carl Zeiss, Gottingen, Germany).

2.5. Fluorescence-activated cell sorting (FACS) analysis

Quantification of PEDV-infected cells upon independent treatment of each SAPK inhibitor was analyzed by flow cytometry. Vero cells were pretreated with SB202190, SP600125, or DMSO for 1 h, infected with PEDV, and subsequently maintained in the presence of vehicle or each inhibitor. Virus-infected cells were trypsinized at 48 hpi and centrifuged at 250*g* (Hanil Centrifuge FLETA 5) for 5 min. The cell pellet was washed with cold washing buffer (1% BSA and 0.1% sodium azide in PBS), and 10^6 cells were resuspended in 1% formaldehyde solution in cold wash buffer for fixation at 4 °C in the dark for 30 min followed by centrifugation and incubation of the pellet in 0.2% Triton X-100 in PBS at 37 °C for 15 min for permeabilization. After centrifugation, the cell pellet was resuspended in a solution of the primary anti-N MAb and the mixture was incubated at 4 °C for 30 min. The cells were washed and allowed to react with an Alexa Fluor 488-conjugated anti-mouse IgG secondary antibody at 4 °C for 30 min in the dark. The stained cells were washed again and analyzed on a FACSAria III flow cytometer (BD Biosciences).

2.6. Time course of SAPK treatment

Vero cells were infected with PEDV at an MOI of 1. At −1, 0, 1, 2, 4, 6, 8, 10, 12, or 24 hpi, inhibitors were added to give the indicated final concentration over the remainder of the time course experiment. The PEDV-infected and inhibitor-treated cells were further maintained and the infection was terminated at 48 hpi by fixing the monolayers with 4% paraformaldehyde for 10 min at RT. The fixed cells were subjected to FACS analysis to assess the presence of PEDV infection as described above.

2.7. Virus titration

Vero cells were PEDV infected and treated with SB202190, SP600125, or DMSO. The culture supernatants were collected at different time points (6, 12, 24, 36, and 48 hpi) and stored at −80 °C. The PEDV titer was determined by plaque assay using Vero cells as described previously (Nam and Lee, 2010) and quantified as plaque-forming units (PFU) per ml.

2.8. Virus internalization assay

An internalization assay was performed as described previously with some modifications (Cai et al., 2007). Briefly, Vero cells grown in 6-well culture plate were pretreated and infected with PEDV at an MOI of 1 at 4 °C for 1 h in the presence of respective compounds. Unbound viruses were then washed with PBS, and the cells were either incubated at 4 °C or 37 °C in the presence of each SAPK inhibitor or DMSO for 1 h, followed by treatment with proteinase K (0.5 mg/ml) at 4 °C for 45 min to remove the bound but uninternalized virus particles. The PEDV-infected cells were then serially diluted in culture medium and added onto fresh Vero cell monolayers in 96-well tissue culture plates. At 48 h post-incubation, internalized viruses were titrated using plaque assay and quantified as PFU per ml.

2.9. Quantitative real-time RT-PCR

Vero cells were incubated with each SAPK inhibitor or DMSO for 1 h prior to infection and then inoculated with PEDV at an MOI of 1 for 1 h at 37 °C. The virus inoculum was subsequently removed and the infected cells were maintained in fresh medium containing SB202190, SP600125, or DMSO for 48 h. Total RNA was extracted from lysates of the infected cells at 48 hpi using TRIzol reagent (Invitrogen) and treated with DNase I (TaKaRa, Otsu, Japan) according to the manufacturer's protocols. The concentrations of the

extracted RNA were measured using a NanoVue spectrophotometer (GE Healthcare). Quantitative real-time RT-PCR was conducted using a Thermal Cycler Dice Real Time System (TaKaRa) with gene-specific primer sets described previously (Kim and Lee, 2013). The RNA levels of viral genes were normalized to that of mRNA for the glyceraldehyde-3-phosphate dehydrogenase (GAPDH) gene, and relative quantities (RQ) of mRNA accumulation were evaluated using the $2^{-\Delta\Delta Ct}$ method. To detect alterations in the genomic RNA and sg mRNA levels in the presence of each SAPK inhibitor during PEDV infection, the results obtained using inhibitor-treated samples were compared to those of DMSO-treated results.

2.10. Northern blotting

Vero cells were pretreated with each inhibitor for 1 h followed by PEDV inoculation and were maintained as described above. Total RNA was extracted from lysates of the infected cells at 48 hpi using TRIzol reagent and treated with DNase I. Northern blotting was conducted by the NorthernMax Kit (Ambion, Austin, TX) according to the manufacturer's instructions. Samples of total RNA (5 μg) were loaded and separated by electrophoresis through Denaturing Gel Buffer-containing 1% agarose gel. The separated total RNA was then transferred to a BrightStar-Plus nylon membrane (Ambion) for 3 h and cross-linked by UV light for 5 min. Pre-hybridization was performed at 42 °C for 40 min followed by detection using the PEDV-specific 3′ UTR probe (5′-GCGGATCTTTAATTACTCGTGCAAAGGTTTAGATGAAAAG-GTACTGCGTTCCCC-3′) or monkey glyceraldehyde-3-phosphate dehydrogenase (GAPDH) (5′-GCCTGGCTGTTAGGTATCGGTGAGG-3′). The blot was hybridized to biotin-labeled oligonucleotide probes in ULTRAhyb reagent at 42 °C overnight and washed twice with low-stringency blocking buffer and wash buffer. Target viral RNAs were detected by the BrightStar BioDetect Kit (Ambion) according to the manufacturer's protocol. The membrane was incubated with alkaline phosphatase-conjugated streptavidin followed by reaction with the chemiluminescent substrate CDP-STAR (Ambion). The overlaid films were obtained by exposure in a dark cassette box in a dark room.

2.11. Annexin V and PI staining assay

Vero cells were pretreated with each inhibitor for 1 h and then mock infected or infected with PEDV at an MOI of 1. The virus-inoculated cells were further propagated in the presence of SB202190 (10 μM), SP600125 (5 μM), or DMSO. Phosphatidylserine exposure was determined by measuring Annexin V binding at the indicated times using an Alexa Fluor 488 Annexin V/Dead Cell Apoptosis Kit (Invitrogen), according to the manufacturer's protocol. In brief, cells were harvested, washed with cold PBS, and suspended in 100 μl 1× annexin-binding buffer. The cells were then incubated with Alexa Fluor 488-conjugated Annexin V and propidium iodide (PI) at RT for 15 min in the dark. Following the incubation period, 400 μl of annexin-binding buffer was added to each sample, and the samples were mixed gently and kept on ice. The fluorescent signals of Annexin V and PI were detected at channels FL-1 and FL-2, respectively, and analyzed using a FACSAria III flow cytometer. Cells negative for PI uptake and positive for Annexin V were considered apoptotic.

2.12. Statistical analysis

All statistical analyses were performed using Student's *t* test, and *P*-values of less than 0.05 were considered statistically significant.

3. Results

3.1. PEDV activates p38 MAPK and JNK1/2

In this study, the roles of the p38 MAPK and JNK pathways in PEDV replication were assessed in the course of PEDV infection. In order to examine the effect of PEDV on the SAPK signaling cascades, the kinetics of p38 and JNK1/2 phosphorylation were monitored by western blot analysis in Vero cells infected with PEDV at an MOI of 1 at different time ponts post-infection. As shown in Fig. 1, only small amounts of activated p38 and JNK1/2 were detected independently in mock-infected Vero cells used as a negative control. Those results were assumed to be background levels of p38 and JNK1/2 phosphorylation (p-p38 and p-JNK1/2), possibly in response to some components of the culture medium. In contrast, PEDV infection stimulated robust phosphorylation of both p38 and JNK1/2 activity up until 36 hpi. The maximal induction was observed at 12 hpi, and then the phosphorylation levels reverted to basal values, or even to levels significantly lower than the basal ones, at 48 hpi (Fig. 1A and C). In addition, comparable activation profiles of p38 and JNK1/2 were observed in cells infected with PEDV at an MOI of 0.1 (data not shown). On the other hand, the degree of p38 phosphorylation was found to be more persistent and much stronger than that of JNK1/2 during PEDV infection. Nevertheless, these results indicated that PEDV infection induces relatively prolonged and durable activation of these two MAPKs. New synthesis of viral proteins was first evident by 12 hpi (Fig. 1A and C), while the maximal phosphorylation status of p38 and JNK1/2 was also seen at this time point, suggesting that p38 and JNK1/2 activation depended on PEDV replication. On the basis of these data, we hypothesized that p38 and JNK1/2 regulation occurred during the late events of viral infection starting the noticeable protein biosynthesis. To verify this hypothesis, we treated Vero cells with equal amounts of UV-irradiated inactivated virus, which can perform viral attachment and internalization but cannot launch viral gene expression (Fig. 1B and D). Unlike infectious PEDV, UV-inactivated PEDV was incapable of triggering p38 and JNK1/2 activation in virus-infected cells. Therefore, infection by inactivated PEDV was insufficient to activate the p38 and JNK signaling pathways, suggesting that initial entry events of viral replication were dispensable for the SAPK activation.

3.2. Activation of p38 MAPK and JNK1/2 regulates PEDV replication

To determine biological relevance of p38 MAPK and JNK1/2 activation for PEDV infection, specific inhibitors of these SAPK signaling pathways were used. Vero cells were pretreated with the p38 inhibitor SB202190 or JNK inhibitor SP600125 at various concentrations or with DMSO (0.5%) as a vehicle control for 1 h prior to infection. Each inhibitor or DMSO was present during the entire period of infection. The cytotoxicity of SAPK inhibitors was determined by the MTT assay in Vero cells. At no dose tested did the inhibitors cause any detectable cell death in Vero cells in this study (data not shown). Viral production was initially measured by monitoring the strength of the cytopathic effect (CPE) after infection and confirmed by immunofluorescence using an anti-N protein MAb at 48 hpi (Fig. 2). In vehicle-treated control cells, a visible CPE appeared at 24 hpi and became predominant by 48 hpi. PEDV N protein-specific staining was markedly pronounced in many cell clusters, indicating infection and spread of the virus to neighboring cells. The inhibitory effects of SB202190 or SP600125 on viral propagation were readily detectable. As shown in Fig. 2A, each inhibitor significantly attenuated PEDV-induced CPE (first panels) and PEDV gene expression (second panels) in a dose-dependent manner. According to quantification of N protein staining results, the proportion (%) of virus-infected cells was noticeably reduced

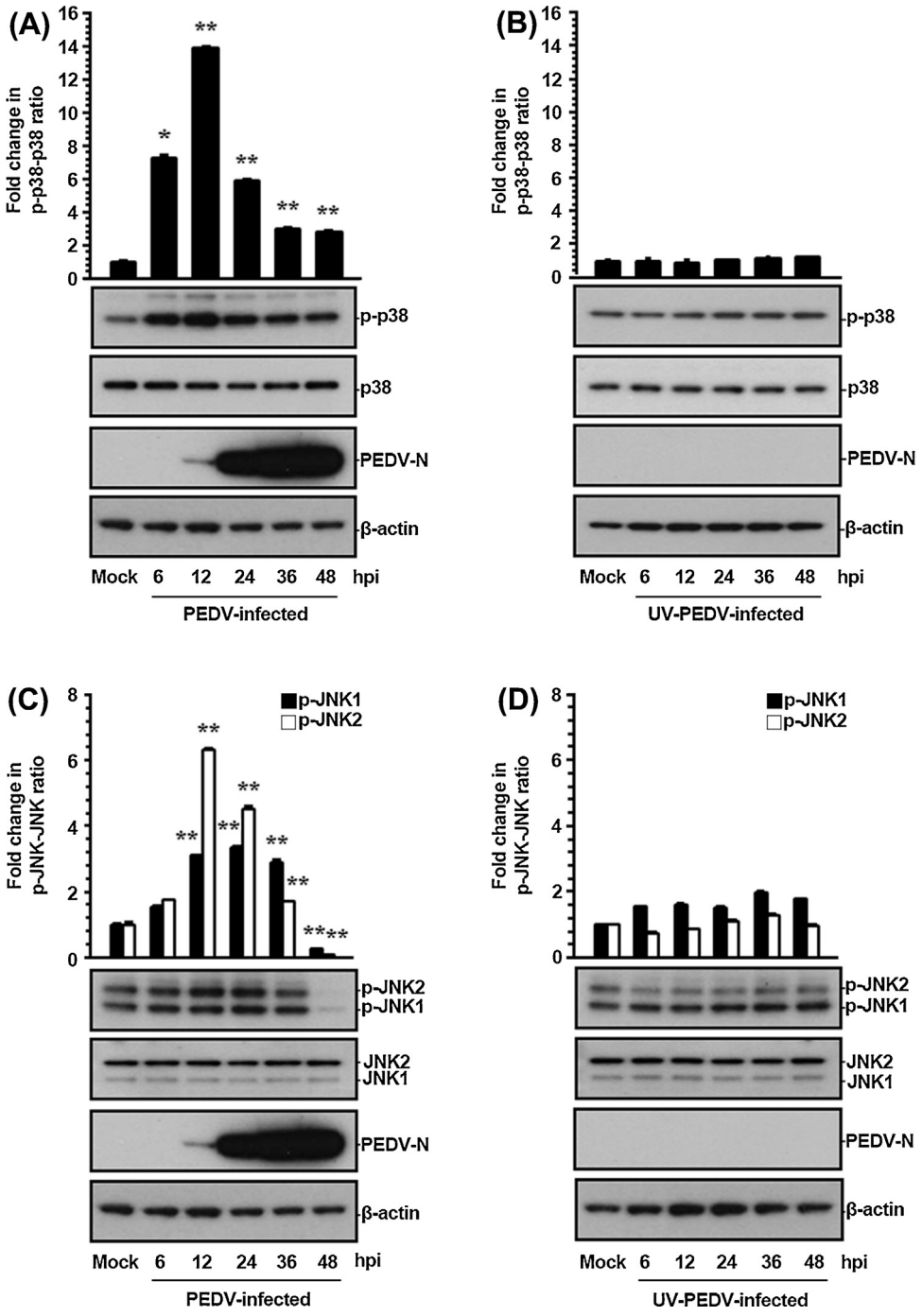

Fig. 1. PEDV activates the p38 MAPK and JNK1/2 signaling pathways in cultured cells. Vero cells were mock infected or infected with PEDV at an MOI of 1 (A and C) or an equal amount of UV-inactivated PEDV (B and D). Whole cell lysates were prepared for the indicated time points following PEDV infection and subjected to western blot analysis with the antibody specific for phosphorylated p38 (p-p38), p38, p-JNK1/2, JNK1/2, or the PEDV N protein. The blot was also reacted with a mouse MAb against b-actin to verify equal protein loading. Fold changes in ratios of p-p38:total p38 and p-JNK1/2:total JNK1/2 compared by densitometry of the corresponding bands using a computer densitometer are plotted. These data are representative of the results of three independent experiments and error bars represent standard deviations. *, $P < 0.05$; **, $P < 0.001$.

during treatment with either SB202190 or SP600125. At the highest concentration used, each drug inhibited viral replication by 85% and 60%, respectively (Fig. 2B). Our data also revealed that SB202190 was significantly more effective in inhibiting PEDV production (a nearly 80% reduction in viral propagation was achieved at the concentration of 5 μM) than SP600125 (a 50% reduction at the same concentration). The discriminative effects of the two inhibitors on PEDV infection indicated that p38 activation is probably more robust and significant than activation of JNK in PEDV-infected cells as described above. To further verify the importance, we determined the activation status of p38 MAPK and JNK1/2 following treatment with the corresponding inhibitor in PEDV-infected cells. The presence of either inhibitor markedly decreased levels of the respective phosphorylated SAPK throughout the PEDV infection: these levels were comparable to those in mock-infected cells (Fig. 2C). This result suggested that the effect of both inhibitors on viral production correlated with the ability of each compound to inhibit p38 MAPK or JNK1/2 phosphorylation. Taken together, these

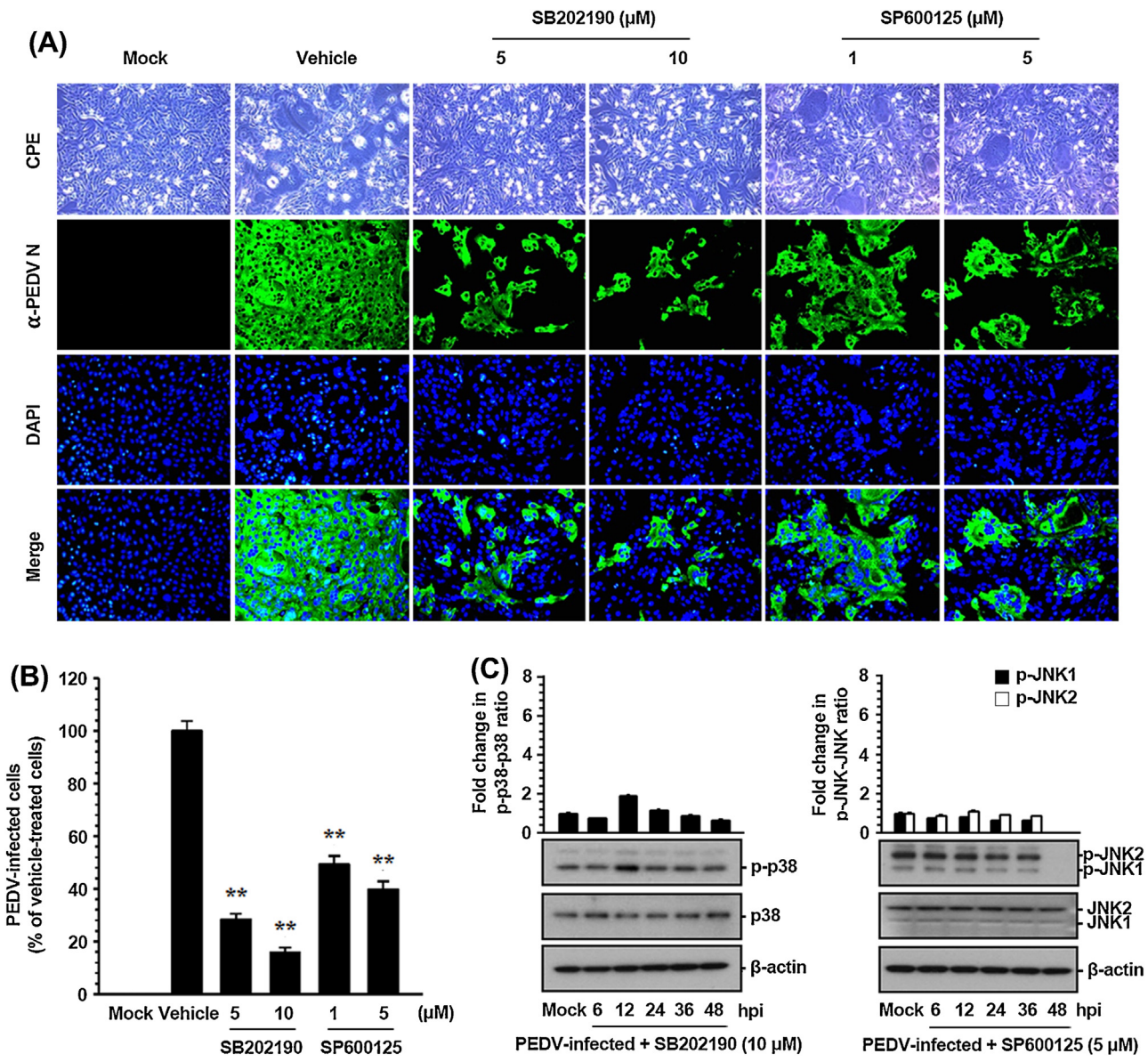

Fig. 2. PEDV propagation is suppressed by inhibition of p38 MAPK and JNK1/2 activation. (A) Vero cells were preincubated with DMSO, SB202190 (5 and 10 μM), or SP600125 (1 and 5 μM) for 1 h prior to infection and were mock-infected or infected with PEDV at an MOI of 1. The virus-infected cells were further maintained for 48 h in the presence of DMSO or inhibitors. PEDV-specific CPEs were monitored daily and were photographed at 48 hpi under an inverted microscope at the magnification of 100× (first panels). For immunostaining, the infected cells were fixed at 48 hpi and incubated with a MAb against the N protein followed by Alexa green-conjugated goat anti-mouse secondary antibody (second panels). The cells were then counterstained with DAPI (third panels) and examined using a fluorescent microscope at 200× magnification. (B) Viral production in the presence of each inhibitor was calculated by measuring the percentage of cells expressing N proteins through flow cytometry. The values shown are representative of three independent experiments, and the error bars represent standard deviations. **, $P < 0.001$. (C) Chemical inhibition of p38 MAPK or JNK activation was quantitated by western blot analysis. Vero cells were pretreated with SB202190 (10 μM) or SP600125 (5 μM) for 1 h prior to infection and were mock-infected or infected with PEDV at an MOI of 1. Whole cell lysates were prepared for the indicated time points after PEDV infection and were subjected to immunoblotting with the corresponding primary antibody. Fold changes in ratios of p-p38:total p38 and p-JNK1/2:total JNK1/2 are plotted. These data are representative of the results of three independent experiments, and the error bars represent standard deviations.

data showed that treatment of cells with these inhibitors specifically hampered activation of SAPKs and accordingly suppressed PEDV propagation, thus suggesting that both p38 MAPK and JNK signaling pathways independently perform a crucial function in PEDV replication.

In addition, the virus yield was determined during treatment with SAPK inhibitors to determine whether endogenous p38 and JNK1/2 activity is necessary for PEDV replication. After the infection, viral supernatants were collected at 48 hpi, and viral titers were measured. As illustrated in Fig. 3A, each inhibitor suppressed the release of viral progeny in a dose-dependent manner. The peak viral titer was $10^{6.8}$ PFU/ml in the DMSO-treated control. The addition of SB202190 or SP600125 at the highest concentration reduced the PEDV titer to $10^{3.9}$ and $10^{4.8}$ PFU/ml, respectively (3- and 2-log reductions as compared to control levels). Examination of the growth kinetics also showed that the overall process of PEDV replication was markedly delayed when the cells were treated with either SB202190 or SP600125 at their respective optimal concentrations (Fig. 3B). Consequently, these findings confirmed that activation of the p38 and JNK pathways is an integral part of successful PEDV replication in Vero cells.

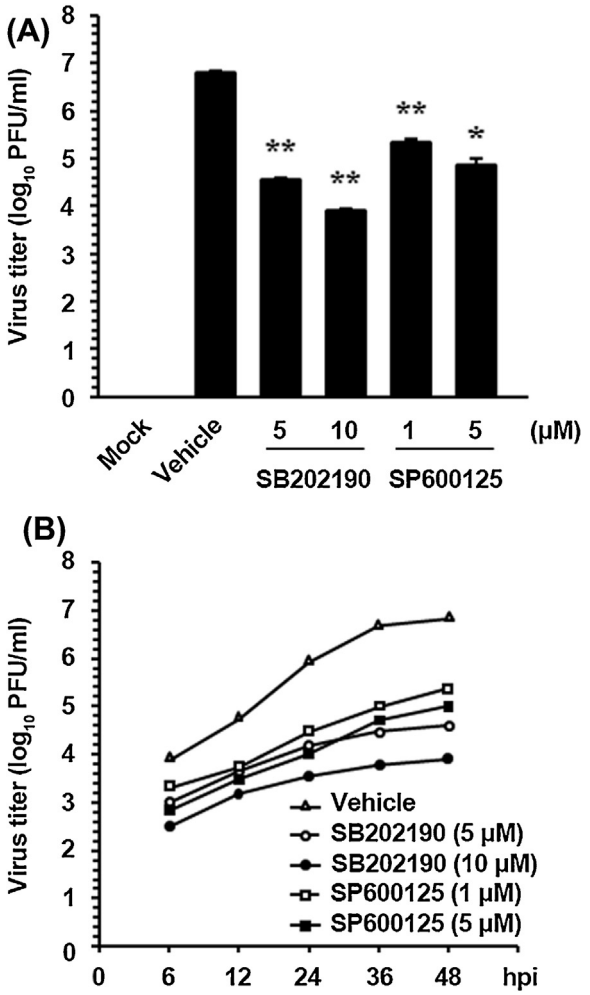

Fig. 3. SAPK inhibitors reduce viral progeny production. (A) Vero cells were pretreated with DMSO, SB202190, or SP600125 for 1 h and were mock or PEDV infected (MOI of 1). Vehicle or each inhibitor was present in the medium throughout the infection. At 48 hpi, the viral supernatants were collected, and viral titers were determined. (B) Growth kinetics of PEDV upon treatment with each inhibitor was assessed exactly as for panel A. At the indicated time points post-infection, culture supernatants were harvested and virus titers were measured. The results are expressed as the mean values from triplicate wells, and the error bars represent standard deviations. *, $P < 0.05$; **, $P < 0.001$.

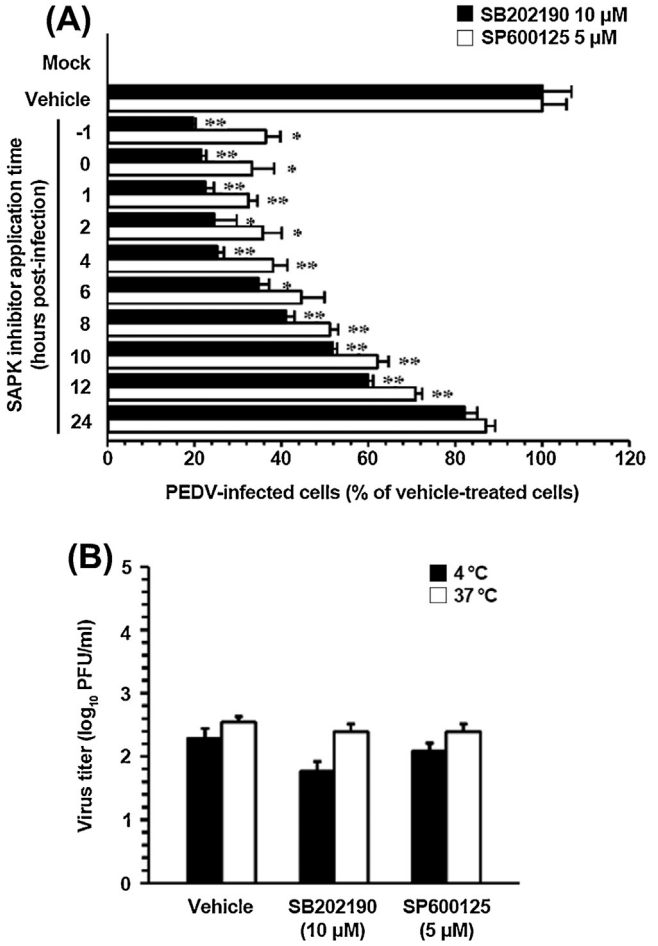

Fig. 4. Activation of p38 MAPK and JNK is required at early stages of PEDV infection but does not affect virus internalization. (A) Vero cells were pretreated with DMSO, SB202190 (5 and 10 μM), or SP600125 (1 and 5 μM) and were mock or PEDV (MOI of 1) infected. At the indicated time points post-infection, each inhibitor was added to attain the intended final concentration. At 48 hpi, the virus-infected cells were fixed, and virus infectivity was determined by measuring the percentage of cells expressing N proteins through FACS. (B) Virus internalization assay. Vero cells were infected at an MOI of 1 at 4 °C for 1 h. After washing with cold PBS, the infected cells were incubated with or without each inhibitor either at 4 °C or 37 °C for an additional hour. Bound but non-internalized viral particles were removed by treatment with proteinase K. The infected cells were then serially diluted and plated onto Vero cells in 96-well tissue culture plates. At 2 days post-incubation, internalized viruses were titrated by a plaque assay. The results are expressed as the mean values from triplicate wells, and the error bars represent standard deviations. *, $P < 0.05$; **, $P < 0.001$.

3.3. *Inhibition of p38 and JNK activation suppresses PEDV replication at early stages of the viral infection but does not influence virus internalization*

To identify the PEDV infection stage at which SAPK inhibitors exerted their action, Vero cells were treated with each inhibitor at different time points post-infection. At 48 hpi, the levels of PEDV replication were measured indirectly by quantifying the cells that expressed the N protein by using flow cytometry (Fig. 4A). Treating the cells with 10 μM SB202190 for up to 4 hpi resulted in a 75% decrease in PEDV infection in comparison with the control levels (DMSO-treated cells). Addition of the inhibitor between 6 and 12 hpi inhibited PEDV replication to 65–40% of control levels. Similarly, treatment with 5 μM SP600125 for up to 4 hpi suppressed the viral infection by 65%, whereas exposure to the inhibitor in the period from 6 to 12 hpi lowered PEDV production levels to 50–30% of the respective control parameter. In contrast, little or no impairment of PEDV propagation was observed when either inhibitor was added at 24 hpi. These data showed that p38 and JNK inhibitors had to be present prior to or during the early period of viral infection to efficiently exert their own antiviral effect. Thus, the importance of SAPK signaling pathways is apparently significant during the early period of PEDV infection.

Next, we sought to identify the step(s) of the replication cycle of PEDV that was specifically targeted by inhibition of p38 and JNK activation. To address this issue, the earliest step, virus entry, was first assessed with an internalization assay upon treatment with each inhibitor. Vero cells were inoculated with PEDV at 4 °C for 1 h to allow for virus attachment and further maintained either at 4 °C or 37 °C to permit virus internalization in the presence of SB202190 (10 μM), SP600125 (5 μM), or DMSO, followed by treatment with proteinase K to remove the remaining viral particles from the cell surface. The serially diluted infected cells were subsequently subjected to an infectious center assay on uninfected Vero cell monolayers, and virus titers were measured 2 days later by a plaque assay (Fig. 4B). Only minimal viral growth was observed in cells maintained at 4 °C, which was likely due to inefficient removal of the bound virus. The titers of PEDV were nearly identical in cells

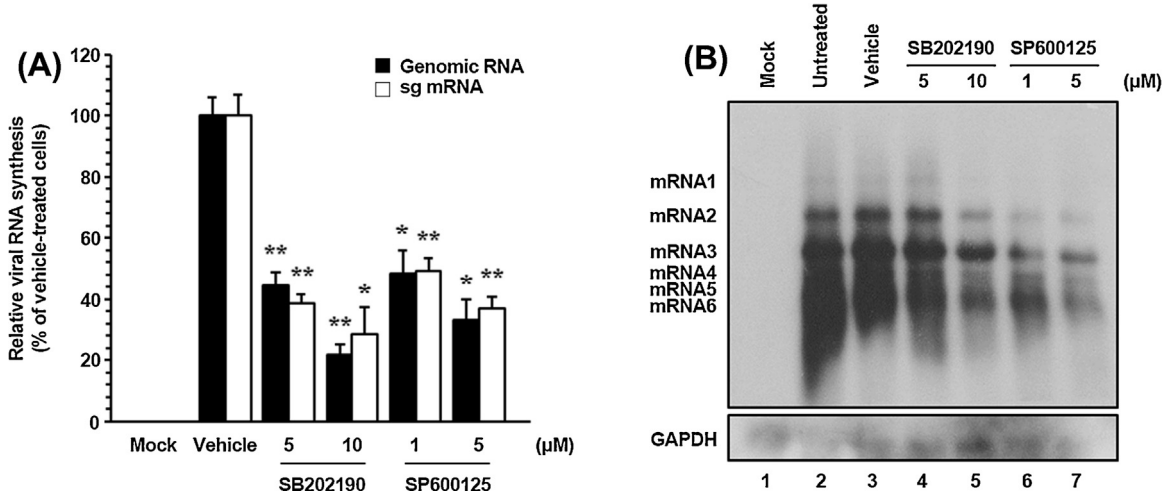

Fig. 5. Pharmacological inhibition of p38 MAPK and JNK activation interferes with viral RNA synthesis. Vero cells pretreated with DMSO, SB202190, or SP600125 were mock-infected or infected with PEDV (MOI of 1) for 1 h and were incubated with either DMSO or each inhibitor. (A) Total cellular RNA was extracted at 48 hpi, and strand-specific viral genomic RNA (black bars) and sg mRNA (white bars) were amplified by quantitative real-time RT-PCR. Viral positive-sense genomic RNA and sg mRNA were normalized to mRNA of monkey GAPDH, and relative quantities (RQ) of mRNA accumulation were evaluated. The results on inhibitor-treated sample were compared with DMSO-treated results. The values shown are representative of the mean from three independent experiments, and the error bars denote standard deviations. *, $P < 0.05$; **, $P < 0.001$. (B) The extracted RNA was also subjected to northern blot analysis using the specific oligonucleotide biotin-labeled probes against the PEDV-specific 3′ UTR probe. Monkey GAPDH was served as an internal control to correct the data for variations in loading during viral RNA quantification. The positions of the genomic RNA and sg mRNAs are indicated next to the gel.

treated with SB202190, SP600125, or vehicle at 37 °C and constituted $10^{2.4}$, $10^{2.4}$, and $10^{2.5}$ PFU/ml, respectively, indicating no differences among these treatments. These results revealed that neither SB202190 nor SP600125 had any inhibitory effect on the virus entry process.

3.4. Treatment with SAPK inhibitors disrupts PEDV RNA and protein biosynthesis

As in the case of other positive-sense RNA viruses, the genome of PEDV promptly serves as a template for viral translation by hijacking the host translational machinery. Early PEDV translation generates the replicase polyproteins that are proteolytically processed into nsps. Subsequently, the nonstructural replicase proteins drive *de novo* synthesis of viral RNA. Therefore, we focused on the post-entry phases of the viral life cycle to determine the functional mechanisms of p38 MAPK and JNK1/2 regulatory effects on PEDV infection. Because PEDV infection produces genomic and subgenomic RNA species, we first tested whether each SAPK inhibitor specifically affected genome replication and sg mRNA transcription. For this purpose, relative levels of both genomic RNA and sg mRNA were assessed by quantitative real-time strand-specific RT-PCR in the presence or absence of the p38 or JNK inhibitors upon PEDV infection. As shown in Fig. 5A, both inhibitors dramatically diminished viral RNA synthesis in a dose-dependent manner. At their highest concentrations, p38 or JNK inhibitors reduced levels of viral genomic RNA and sg mRNA by 80–67% and 72–63%, respectively, as compared to those observed in the DMSO-treated cells. The reductions in viral RNA levels caused by either inhibitor did not reflect nonspecific inhibition of transcription because internal control GAPDH mRNA level remained unchanged in all samples (data not shown). The impairment of PEDV transcription in the presence of each inhibitor was further confirmed by northern blot analysis (Fig. 5B). In untreated (lane 2) or vehicle-treated (lane 3) virus-infected cells, PEDV RNA synthesis was distinctly observed. Consistent with the real-time RT-PCR data, a significant reduction in RNA-synthesizing activity occurred dose-dependently after treatment with SB202190 (lanes 4 and 5) or SP600125 (lanes 6 and 7). Taken together, these results indicated that SAPK inhibitors specifically suppressed synthesis of the PEDV genomic RNA and sg mRNA.

Since PEDV structural proteins are translated late in the cycle from their respective sg mRNA transcripts, it is conceivable that suppression of viral protein expression is a cascade-like consequence of inhibition of viral RNA synthesis. Thus, we then examined whether viral protein translation was influenced by inhibition of p38 and JNK activation. To accomplish this, Vero cells were exposed to each inhibitor for 1 h prior to infection and the inhibitors remained in the culture medium during infection and post-infection stages. The expression level of the PEDV N protein in the presence of each inhibitor or DMSO was evaluated at 48 hpi by western blot analysis. Each pharmacological inhibitor had a detrimental effect on viral protein production at different concentrations (Fig. 6). Densitometric analysis of the western blots revealed that intracellular expression of the N protein was effectively prevented by both inhibitors and that SB202190 and SP600125 inhibited N protein production by approximately 80% and 60% at the highest concentrations, respectively (Fig. 6A). Furthermore, the mean fluorescence intensity corresponding to PEDV N expression was significantly reduced in the presence of each inhibitor (Fig. 6B). These data suggested that the suppressive effect of each SAPK inhibitor on viral protein expression resulted from its specific preceding action on viral RNA biosynthesis during PEDV replication.

3.5. Activation of p38 and JNK is not related to PEDV-induced apoptosis

The p38 MAPK and JNK pathways are activated in response to a variety of stressors and have been implicated in numerous cellular events. Accumulating evidence unravels that activation of p38 and JNK signaling is associated with a cell cycle arrest and apoptosis induction (Sui et al., 2014). Moreover, PEDV infection can mediate apoptotic cell death *in vitro* and *in vivo* and thereby facilitate viral replication and pathogenesis (Kim and Lee, 2014). Therefore, we anticipated that the p38 MAPK and JNK cascades play a role in PEDV-induced apoptosis during viral replication. To determine whether p38 and JNK activation is required for induction of apo-

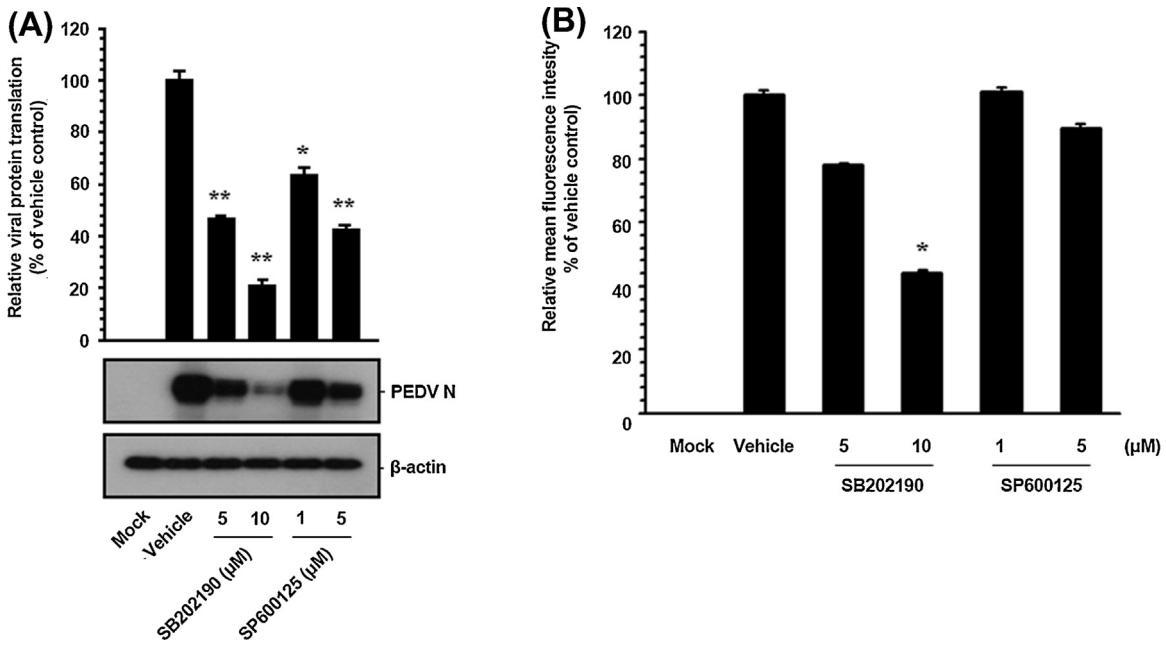

Fig. 6. Pharmacological inhibition of p38 MAPK and JNK activation impairs viral protein translation. Inhibitor-treated Vero cells were mock-infected or infected with PEDV (MOI of 1) for 1 h and were then cultivated in the presence or absence of each inhibitor. (A) At 48 hpi, cellular lysates were prepared, resolved by SDS-PAGE, transferred to a nitrocellulose membrane, and immunoblotted with the antibody against the PEDV N protein. The blot was also reacted with a mouse MAb against β-actin to verify equal protein loading. Each viral protein expression was quantitatively analyzed by densitometry in terms of the density value relative to the β-actin gene, and inhibitor-treated sample results were compared to DMSO-control results. (B) The cells were also subjected to FACS analysis using the anti-PEDV N antibody to determine the mean fluorescence intensity for viral protein expression. The values shown are representative of the mean from three independent experiments, and the error bars denote standard deviations. *, $P < 0.05$; **, $P < 0.001$.

ptosis by PEDV infection, PEDV-triggered apoptosis was analyzed in the presence or absence of each SAPK inhibitor by using flow cytometry with Annexin V and PI staining. Vero cells were treated with DMSO or each compound at indicated concentrations and then infected with PEDV. At various time points post-infection, the treated and infected cells were stained with Annexin V and PI and then examined using FACS flow cytometry to measure fractions of live, apoptotic, and dead cells (Fig. 7 A). Neither the vehicle nor the inhibitors caused significant apoptosis in our experimental settings. As expected, PEDV infection in the presence of DMSO caused substantial apoptosis (Annexin V positive/PI negative) at 6 hpi, and the percentage of early apoptotic cells gradually increased with infection time. Nonetheless, chemical inhibition of p38 MAPK and JNK activation was incapable of protecting the cells from PEDV-triggered apoptosis. The fraction of early apoptotic cells in cultures treated with either SB202190 or SP600125 was comparable to that among vehicle-treated cells in the course of PEDV infection (Fig. 7B). Furthermore, mitochondrial-to-nuclear translocation of AIF, a hallmark of PEDV-mediated apoptosis, persisted in the presence of each SAPK inhibitor (Kim and Lee, 2014; Fig. 7C). Taken together, our data indicated that the p38 MAPK and JNK signaling pathways are not linked to PEDV-mediated apoptosis.

4. Discussion

Numerous viruses have developed an ability to take advantage of host signaling pathways to maximize viral replication. Among a variety of transduction signals, SAPK pathways involving p38 MAPK and JNK1/2 play multiple pivotal roles in a wide range of cellular functions governing cell fate and in regulation of viral multiplication. The interplay between SAPK cascades and viral activities appears to be a general feature of an optimal viral infection process and a global strategy that benefits viral replicative machinery. Despite decades of research, little is deciphered about the intracellular signaling pathways involved in PEDV infection and pathogenesis. The present study showed for the first time that the p38 MAPK and JNK1/2 pathways are required independently for efficient PEDV replication in cultured cells. In this report, we exhibited that PEDV induces strong activation of these two SAPKs in vitro, revealing significance of the SAPK cascade in the course of PEDV infection. Treatment with each SAPK inhibitor greatly impaired PEDV propagation. Moreover, pharmacological inhibition of p38 or JNK activation significantly attenuated viral replication during post-entry steps according to the observed overall down-regulation of viral protein expression, viral RNA synthesis, and progeny release. Thus, it appears that the p38 MAPK and JNK1/2 signaling pathways are manipulated by PEDV to ensure competent viral reproduction in target cells.

In contrast to infectious PEDV, the UV-inactivated virus failed to stimulate phosphorylation of p38 MAPK and JNK1/2; therefore, the activation kinetics was not mediated by virus entry steps such as the virus-receptor interaction and uncoating. On the other hand, it was reported that UV-irradiated PEDV can induce activation of the ERK1/2 pathway, augmenting ERK1/2 phosphorylation to levels comparable to those achieved by the un-irradiated infectious virus. In that case, ERK activation was likely triggered by the virus entry process (Kim and Lee, 2015). Furthermore, robust ERK1/2 activity was found to be gradually induced in PEDV-infected cells up to 12 hpi, and thereafter, to progressively decline. These previous findings suggest that activation of ERK1/2 occurs independently of maximal PEDV replication and is stimulated in the initial round of the viral replication cycle. On the other hand, productive growth of PEDV commenced at 12 hpi, as determined by the presence of a considerable amount of the viral protein. This phenomenon temporally correlated with up-regulation of p38 MAPK and JNK1/2 phosphorylation status observed during that period and a subsequent reduction in their activation to basal levels, or even below them after 36 hpi. The one-step growth curve indicated that the eclipse period lasted until 6 hpi and immediately after this, a productive infection cycle actively proceeded, and progeny viruses became

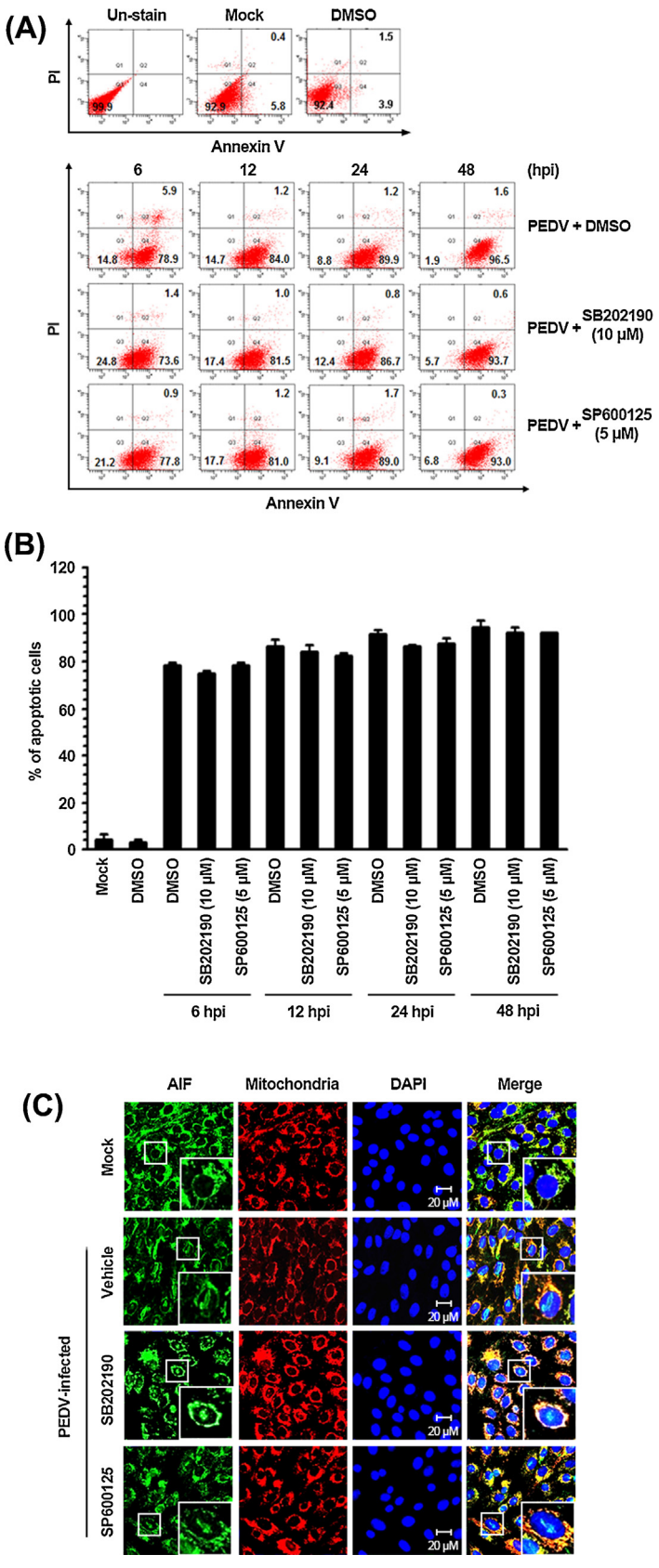

Fig. 7. Inhibition of SAPK activation does not influence PEDV-induced apoptosis. Vero cells were treated with DMSO, SB202190 (10 μM), or SP600125 (5 μM) for 1 h prior to infection and then mock-infected or infected with PEDV (MOI of 1) in the presence of either DMSO or each inhibitor. (A) The cells were harvested at the indicated time points, dually labeled with Annexin V and PI, and subjected to FACS analysis. The lower left quadrants represent intact cells (Annexin V negative/PI negative); the lower right quadrants represent early apoptotic cells (Annexin V positive/PI negative); the upper right quadrants indicate late apoptotic and/or necrotic cells (Annexin V positive/PI positive); and the upper left quadrants indicate necrotic cells (Annexin V negative/PI positive). (B) The percentage of apoptotic cells (Annexin V positive/PI negative and Annexin V positive/PI positive) was plotted. The graph represents mean values from three independent experiments, and the error bars denote standard deviations. (C) The treated and infected cells were also labeled with MitoTracker Red CMXRos (Red), fixed, and incubated with an anti-AIF antibody (green). AIF nuclear translocation is represented by the merged AIF and DAPI signals (turquoise), and residual mitochondrial colocalization is indicated by the merged AIF and mitochondrial marker (yellow). The inset images are enlarged versions of parts of a picture. (For interpretation of the references to color in this figure legend, the reader is referred to the web version of this article.)

detectable. Although the exact mechanism of SAPK activation following PEDV infection was not determined in the present study, it is tempting to speculate that p38 and JNK1/2 activation directly depends on efficient PEDV production during the late events of viral infection. In addition, because p38 and JNK are potently induced by pro-inflammatory cytokines, another possibility is that activation of the p38 MAPK and JNK1/2 signaling pathways is indirectly triggered by induction of cytokines upon PEDV infection rather than by active viral replication per se.

Results of the present study raise a question regarding the definite role of activated SAPKs during PEDV infection. A conceivable explanation of how p38 MAPK and/or JNK activation controls PEDV infection is that the SAPK pathways regulate viral replication directly or indirectly. Treatment of PEDV-infected cells with either a p38 or JNK inhibitor significantly suppressed post-internalization cascades of the viral replication cycle, including viral RNA synthesis, protein expression, and progeny virus release. Empirical evidence indicates that positive-sense RNA virus RdRps are phosphoproteins activated by host proteins, such as kinases, suggesting that viral RNA replication is regulated by phosphorylation of the polymerase protein (Jakubiec and Jupin, 2007; Moser and Schultz-Cherry, 2008). Thus, p38 MAPK and JNK activity may be relevant to phosphorylation and resulting stabilization of the PEDV RdRp (nsp12), which may be indispensable for optimal viral RNA synthesis. Apoptotic cell death is known to be modulated by the p38 MAPK and JNK cellular stress pathways (Kyriakis and Avruch, 2001; Wada and Penninger, 2004). Several viruses can trigger activation of p38 MAPK and/or JNK, which mediates apoptosis via either intrinsic or extrinsic pathways, and thereby contributes to viral replication (Padhan et al., 2008; Sumbayev and Yasinska, 2006; Wang et al., 2004; Wei et al., 2009). We previously demonstrated that PEDV promotes apoptotic cell death *in vitro* and *in vivo* to support viral infection and pathogenesis (Kim and Lee, 2014). In contrast, the present study showed no crosstalk between SAPK activation and apoptosis during PEDV infection. This result was expected because neither cytochrome *c* release nor caspase activation were found to participate in the PEDV-induced apoptosis pathway (Kim and Lee, 2014). Alternatively, SAPK activation may be indirectly involved in PEDV infection by stimulating other cascades to modify expression of immune system-related genes and other proteins (e.g., cellular transcription factors) necessary for maximal viral propagation. Indeed, viral infection can activate the p38 MAPK and/or JNK pathways and thereby regulate production of various cytokines (Huang et al., 2011; Lee and Lee, 2012; Regan et al., 2009; Yu et al., 2009). Moreover, we were unable to block viral replication completely during pharmacological inhibition under our experimental conditions. Therefore, if p38 MAPK and/or JNK activity exert an indirect influence, SAPK signaling may be one of the pivotal viral mechanisms for control of expression of immune-response genes in order to favor successful survival and spread of the virus in the natural host.

In conclusion, our findings revealed that PEDV activates both p38 MAPK and JNK1/2 in the late period of viral infection in cultured

cells. We found that activation of these two kinases is indispensable for efficient PEDV replication *in vitro*. However, specific viral processes or components responsible for the p38 and JNK activation have yet to be determined. Although our data showed an impairment of viral RNA biosynthesis and of viral protein production after inhibition of SAPK activation, the precise mechanism by which virus-activated p38 MAPK and JNK modulate the PEDV replication cycle during infection is still unclear and therefore, will become the subject of our future studies. Thus, a better understanding of the specific function of p38 MAPK and JNK1/2 activation in the replication of PEDV will provide valuable insights into the molecular biology and pathogenesis of PEDV.

Acknowledgment

This research was supported by Basic Science Research Program through the National Research Foundation of Korea (NRF) funded by the Ministry of Education, Science and Technology (NRF-2012R1A1A2039746).

References

Boniotti, M.B., Papetti, A., Lavazza, A., Alborali, G., Sozzi, E., Chiapponi, C., Faccini, S., Bonilauri, P., Cordioli, P., Marthaler, D., 2016. Porcine epidemic diarrhea virus and discovery of a recombinant swine enteric coronavirus, Italy. Emerg. Infect. Dis. 22, 83–87.

Cai, Y., Liu, Y., Zhang, X., 2007. Suppression of coronavirus replication by inhibition of the MEK signaling pathway. J. Virol. 81, 446–456.

Chen, J.F., Sun, D.B., Wang, C.B., Shi, H.Y., Cui, X.C., Liu, S.W., Qiu, H.J., Feng, L., 2008. Molecular characterization and phylogenetic analysis of membrane protein genes of porcine epidemic diarrhea virus isolates in China. Virus Genes 36, 355–364.

Debouck, P., Pensaert, M., 1980. Experimental infection of pigs with a new porcine enteric coronavirus, CV 777. Am. J. Vet. Res. 41, 219–223.

Dong, C., Davis, R.J., Flavell, R.A., 2002. MAP kinases in the immune response. Annu. Rev. Immunol. 20, 55–72.

Duarte, M., Tobler, K., Bridgen, A., Rasschaert, D., Ackermann, M., Laude, H., 1994. Sequence analysis of the porcine epidemic diarrhea virus genome between the nucleocapsid and spike protein genes reveals a polymorphic ORF. Virology 198, 466–476.

Georgopoulou, U., Caravokiri, K., Mavromara, P., 2003. Suppression of the ERK1/2 signaling pathway from HCV NS5A protein expressed by herpes simplex recombinant viruses. Arch. Virol. 148, 237–251.

Grasland, B., Bigault, L., Bernard, C., Quenault, H., Toulouse, O., Fablet, C., 2015. Complete genome sequence of a porcine epidemic diarrhea S gene indel strain isolated in France in December 2014. Genome Announc. 3, e00535.

Greber, U.F., 2002. Signalling in viral entry. Cell Mol. Life Sci. 59, 608–626.

Hanke, D., Jenckel, M., Petrov, A., Ritzmann, M., Stadler, J., Akimkin, V., 2015. Comparison of porcine epidemic diarrhea viruses from Germany and the United States, 2014. Emerg. Infect. Dis. 21, 493–496.

Hofmann, M., Wyler, R., 1988. Propagation of the virus of porcine epidemic diarrhea in cell culture. J. Clin. Microbiol. 26, 2235–2239.

Huang, X., Huang, Y., OuYang, Z., Cai, J., Yan, Y., Qin, Q., 2011. Roles of stress-activated protein kinases in the replication of Singapore grouper iridovirus and regulation of the inflammatory responses in grouper cells. J. Gen. Virol. 92, 1292–1301.

Jakubiec, A., Jupin, I., 2007. Regulation of positive-strand RNA virus replication: the emerging role of phosphorylation. Virus Res. 129, 73–79.

Kim, Y., Lee, C., 2013. Ribavirin efficiently suppresses porcine nidovirus replication. Virus Res. 171, 44–53.

Kim, Y., Lee, C., 2014. Porcine epidemic diarrhea virus induces caspase-independent apoptosis through activation of mitochondrial apoptosis-inducing factor. Virology 460–461, 180–193.

Kim, Y., Lee, C., 2015. Extracellular signal-regulated kinase (ERK) activation is required for porcine epidemic diarrhea virus replication. Virology 484, 181–193.

Kocherhans, R., Bridgen, A., Ackermann, M., Tobler, K., 2001. Completion of the porcine epidemic diarrhoea coronavirus (PEDV) genome sequence. Virus Genes 23, 137–144.

Kweon, C.H., Kwon, B.J., Jung, T.S., Kee, Y.J., Hur, D.H., Hwang, E.K., Rhee, J.C., An, S.H., 1993. Isolation of porcine epidemic diarrhea virus (PEDV) in Korea. Korean J. Vet. Res. 33, 249–254.

Kyriakis, J.M., Avruch, J., 2001. Mammalian mitogen-activated protein kinase signal transduction pathways activated by stress and inflammation. Physiol. Rev. 81, 807–869.

Lai, C.C., Jou, M.J., Huang, S.Y., Li, S.W., Wan, L., Tsai, F.J., Lin, C.W., 2007. Proteomic analysis of up-regulated proteins in human promonocyte cells expressing severe acute respiratory syndrome coronavirus 3C-like protease. Proteomics 7, 1446–1460.

Lee, Y.J., Lee, C., 2010. Porcine reproductive and respiratory syndrome virus replication is suppressed by inhibition of the extracellular signal-regulated kinase (ERK) signaling pathway. Virus Res. 152, 50–58.

Lee, Y.J., Lee, C., 2012. Stress-activated protein kinases are involved in porcine reproductive and respiratory syndrome virus infection and modulate virus-induced cytokine production. Virology 427, 80–89.

Lee, S., Lee, C., 2014. Outbreak-related porcine epidemic diarrhea virus strains similar to US strains South Korea, 2013. Emerg. Infect. Dis. 20, 1223–1226.

Lee, C., 2015. Porcine epidemic diarrhea virus: an emerging and re-emerging epizootic swine virus. Virol. J. 12, 193.

Li, W., Li, H., Liu, Y., Pan, Y., Deng, F., Song, Y., Tang, X., He, Q., 2012. New variants of porcine epidemic diarrhea virus China, 2011. Emerg. Infect. Dis. 8, 1350–1353.

Lim, B., Nam, J., Gil, C., Yun, S., Choi, J., Kim, D., Jeon, E., 2005. Coxsackievirus B3 replication is related to activation of the late extracellular signal-regulated kinase (ERK) signal. Virus Res. 113, 153–157.

Lin, C.N., Chung, W.B., Chang, S.W., Wen, C.C., Liu, H., Chien, C.H., Chiou, M.T., 2014. US-like strain of porcine epidemic diarrhea virus outbreaks in Taiwan, 2013–2014. J. Vet. Med. Sci. 76, 1297–1299.

Marjuki, H., Alam, M.I., Ehrhardt, C., Wagner, R., Planz, O., Klenk, H.D., Ludwig, S., Pleschka, S., 2006. Membrane accumulation of influenza A virus hemagglutinin triggers nuclear export of the viral genome via protein kinase Cα-mediated activation of ERK signaling. J. Biol. Chem. 281, 16707–16715.

Mesquita, J.R., Hakze-van der Honing, R., Almeida, A., Lourenço, M., van der Poel, W.H., Nascimento, M.S., 2015. Outbreak of porcine epidemic diarrhea virus in Portugal, 2015. Transbound. Emerg. Dis. 62, 586–588.

Mori, I., Goshima, F., Koshizuka, T., Koide, N., Sugiyama, T., Yoshida, T., Yokochi, T., Nishiyama, Y., Kimura, Y., 2003. Differential activation of the c-Jun N-terminal kinase/stress-activated protein kinase and p38 mitogen-activated protein kinase signal transduction pathways in the mouse brain upon infection with neurovirulent influenza A virus. J. Gen. Virol. 84, 2401–2408.

Moser, L.A., Schultz-Cherry, S., 2008. Suppression of astrovirus replication by an ERK1/2 inhibitor. J. Virol. 82, 7475–7482.

Nam, E., Lee, C., 2010. Contribution of the porcine aminopeptidase N (CD13) receptor density to porcine epidemic diarrhea virus infection. Vet. Microbiol. 144, 41–50.

Padhan, K., Minakshi, R., Towheed, M.A., Jameel, S., 2008. Severe acute respiratory syndrome coronavirus 3a protein activates the mitochondrial death pathway through p38 MAP kinase activation. J. Gen. Virol. 89, 1960–1969.

Pan, H., Xie, J., Ye, F., Gao, S.J., 2006. Modulation of Kaposi's sarcoma-associated herpesvirus infection and replication by MEK/ERK, JNK, and p38 multiple mitogen-activated protein kinase pathways during primary infection. J. Virol. 80, 5371–5382.

Pensaert, M.B., de Bouck, P., 1978. A new coronavirus-like particle associated with diarrhea in swine. Arch. Virol. 58, 243–247.

Pensaert, M.B., Debouck, P., Reynolds, D.J., 1981. An immunoelectron microscopic and immunofluorescent study on the antigenic relationship between the coronavirus-like agent CV 777, and several coronaviruses. Arch. Virol. 68, 45–52.

Puranaveja, S., Poolperm, P., Lertwatcharasarakul, P., Kesdaengsakonwut, S., Boonsoongnern, A., Urairong, K., Kitikoon, P., Choojai, P., Kedkovid, R., Teankum, K., Thanawongnuwech, R., 2009. Chinese-like strain of porcine epidemic diarrhea virus, Thailand. Emerg. Infect. Dis. 15, 1112–1115.

Rahaus, M., Desloges, N., Wolff, M.H., 2004. Replication of varicella-zoster virus is influenced by the levels of JNK/SAPK and p38/MAPK activation. J. Gen. Virol. 85, 3529–3540.

Regan, A.D., Cohen, R.D., Whittaker, G.R., 2009. Activation of p38 MAPK by feline infectious peritonitis virus regulates pro-inflammatory cytokine production in primary blood-derived feline mononuclear cells. Virology 384, 135–143.

Roux, P.P., Blenis, J., 2004. ERK and p38 MAPK-activated protein kinases: a family of protein kinases with diverse biological functions. Microbiol. Mol. Biol. Rev. 68, 320–344.

Saif, L.J., Pensaert, M.B., Sestack, K., Yeo, S.G., Jung, K., 2012. Coronaviruses. In: Straw, B.E., Zimmerman, J.J., Karriker, L.A., Ramirez, A., Schwartz, K.J., Stevenson, G.W. (Eds.), Diseases of Swine. Wiley-Blackwell Ames, pp. 501–524.

Schümann, M., Dobbelstein, M., 2006. Adenovirus-induced extracellular signal-regulated kinase phosphorylation during the late phase of infection enhances viral protein levels and virus progeny. Cancer Res. 66, 1282–1288.

Shaul, Y.D., Seger, R., 2007. The MEK/ERK cascade: from signaling specificity to diverse functions. Biochim. Biophys. Acta 1773, 1213–1226.

Si, X., Luo, H., Morgan, A., Zhang, J., Wong, J., Yuan, J., Esfandiarei, M., Gao, G., Cheung, C., McManus, B.M., 2005. Stress-activated protein kinases are involved in coxsackievirus B3 viral progeny release. J. Virol. 79, 13875–13881.

Steinrigl, A., Revilla Fernández, S., Stoiber, F., Pikalo, J., Sattler, T., Schmoll, F., 2015. First detection, clinical presentation and phylogenetic characterization of porcine epidemic diarrhea virus in Austria. BMC Vet. Res. 11, 310.

Stevenson, G.W., Hoang, H., Schwartz, K.J., Burrough, E.R., Sun, D., Madson, D., Cooper, V.L., Pillatzki, A., Gauger, P., Schmitt, B.J., Koster, L.G., Killian, M.L., Yoon, K.J., 2013. Emergence of *Porcine epidemic diarrhea virus* in the United States: clinical signs, lesions, and viral genomic sequences. J. Vet. Diagn. Invest. 25, 649–654.

Sui, Y., Zhao, Z., Liu, R., Cai, B., Fan, D., 2014. Adenosine monophosphate-activated protein kinase activation enhances embryonic neural stem cell apoptosis in a mouse model of amyotrophic lateral sclerosis. Neural Regen. Res. 9, 1770–1778.

Sumbayev, V.V., Yasinska, I.M., 2006. Role of MAP kinase-dependent apoptotic pathway in innate immune responses and viral infection. Scand. J. Immunol. 63, 391–400.
Sun, R.Q., Cai, R.J., Chen, Y.Q., Liang, P.S., Chen, D.K., Song, C.X., 2012. Outbreak of porcine epidemic diarrhea in suckling piglets,China. Emerg. Infect. Dis. 18, 161–163.
Suzuki, T., Murakami, S., Takahashi, O., Kodera, A., Masuda, T., Itoh, S., Miyazaki, A., Ohashi, S., Tsutsui, T., 2015. Molecular characterization of pig epidemic diarrhoea viruses isolated in Japan from 2013 to 2014. Infect. Genet. Evol. 36, 363–368.
Takahashi, K., Okada, K., Ohshima, K., 1983. An outbreak of swine diarrhea of a new-type associated with coronavirus-like particles in Japan. Jpn. J. Vet. Sci. 45, 829–832.
Theuns, S., Conceição-Neto, N., Christiaens, I., Zeller, M., Desmarets, L.M., Roukaerts, I.D., 2015. Complete genome sequence of a porcine epidemic diarrhea virus from a novel outbreak in Belgium, January 2015. Genome Announc. 3, e00506.
Tibbles, L.A., Woodgett, J.R., 1999. The stress-activated protein kinase pathways. Cell Mol. Life Sci. 55, 1230–1254.
Wada, T., Penninger, J.M., 2004. Mitogen-activated protein kinases in apoptosis regulation. Oncogene 23, 2838–2849.
Wang, W.H., Grégori, G., Hullinger, R.L., Andrisani, O.M., 2004. Sustained activation of p38 mitogen-activated protein kinase and c-Jun N-terminal kinase pathways by hepatitis B virus X protein mediates apoptosis via induction of Fas/FasL and tumor necrosis factor (TNF) receptor 1/TNF-alpha expression. Mol. Cell Biol. 24, 10352–10365.
Wang, J., Shen, Y.H., Utama, B., Wang, J., LeMaire, S.A., Coselli, J.S., Vercellotti, G.M., Wang, X.L., 2006. HCMV infection attenuates hydrogen peroxide induced endothelial apoptosis-involvement of ERK pathway. FEBS Lett. 580, 2779–2787.
Wei, L., Liu, J., 2009. Porcine circovirus type 2 replication is impaired by inhibition of the extracellular signal-regulated kinase (ERK) signaling pathway. Virology 386, 203–209.
Wei, L., Zhu, Z., Wang, J., Liu, J., 2009. JNK and p38 mitogen-activated protein kinase pathways contribute to porcine circovirus type 2 infection. J. Virol. 83, 6039–6047.
Yu, D., Zhu, H., Liu, Y., Cao, J., Zhang, X., 2009. Regulation of proinflammatory cytokine expression in primary mouse astrocytes by coronavirus infection. J. Virol. 83, 12204–12214.
Zampieri, C.A., Fortin, J.F., Nolan, G.P., Nabel, G.J., 2007. The ERK mitogen-activated protein kinase pathway contributes to Ebloa virus glycoprotein-induced cytotoxicity. J. Virol. 81, 1230–1240.